Colloid and Polymer Science (2020) 298:595–602
https://doi.org/10.1007/s00396-020-04651-2

ORIGINAL CONTRIBUTION

Determination of dynamic wetting behavior using different methods

Junchao Wang [1,2] · Yijun Cao [1,3] · Guosheng Li [3] · Yingwei Wang [1,2] · Shulei Li [1,2] · Yinfei Liao [1,2]

Received: 7 February 2020 / Revised: 27 March 2020 / Accepted: 30 March 2020 / Published online: 6 April 2020

Abstract

Wetting and dewetting are ubiquitous phenomena in nature and industrial applications; thus, it is of great significance to study their dynamic behavior from the perspective of fundamental and applied viewpoints. In this paper, the dynamic wetting behavior of deionized water and oleic acid on smooth hydrophobic surfaces (Teflon) was studied using the Wilhelmy plate–dipping method and the droplet-spreading method, respectively. The former method was used to investigate the dependence of advancing contact angle, receding contact angle and contact angle hysteresis on capillary number, and contact line velocity, and the scaling behavior of the dynamic contact angle was examined. Results showed that for all the wetting systems studied, the advancing contact angle increased monotonically with the rise of capillary number and contact line velocity, while the receding contact angle exhibited an opposite trend, and the hysteresis of contact angle was found to be dependent of capillary number. Besides, the scaling behaviors of advancing contact angle and receding contact angle were found to follow Cox–Voinov–Tanner's scaling law. The latter method suggested that the variations of dynamic contact angle and spreading radius with time could be well described by the expressions, $\theta(t) = \theta_{eq} + a * \exp(-t/m)(a > 0)$ and $R(t) = R_{eq} + a * \exp(-t/m)(a < 0)$, respectively.

Keywords Dynamic wetting behavior · Wilhelmy plate–dipping method · Droplet-spreading method · Dynamic contact angle · Contact angle hysteresis

Introduction

Wetting or dewetting is one of the most important surface properties of a solid; it is commonly encountered in nature, such as water droplet rolling on a lotus leaf [1], raindrop rolling away from butterfly wings rather than toward its body [2], spider silk collecting water due to surface energy gradient and asymmetric Laplace pressure [3], and desert lizards utilizing scale hinges to convergent or transport water for drinking [4]. These unique surfaces of the natural creatures with particular wetting and nonwetting property contribute to creating new technologies and improving people's life [5, 6]. For example, the self-cleaning effect of lotus leaf brings us abundant inspiration for designing functional surfaces with specific nonwetting characteristics through a combination of surface chemical compositions and surface roughness.

Over the past few decades, the basic principle of static wetting phenomenon has been deeply studied [7, 8]; however, the dynamic wetting process, particularly in practical applications, remains not well understood [9]. Recent years, researches on dynamic wetting behavior have been performed experimentally, theoretically and numerically, and great achievements have been obtained [5, 10–12]. It is well known that the Wilhelmy plate–dipping method and the droplet-spreading method are two the common research methods of wetting dynamics. Many significant theoretical models, such as hydrodynamic model (HD) [13, 14], molecular-kinetic theory model (MKT) [15], and combined molecular-hydrodynamic model [16], are proposed to explain the relationship between dynamic contact angle and contact line velocity using the Wilhelmy plate–dipping method. Recently, Karim et al. [17] experimentally studied the dynamic wetting

✉ Yijun Cao
caoyj@cumt.edu.cn

✉ Guosheng Li
lgscumt@163.com

[1] Chinese National Engineering Research Center of Coal Preparation and Purification, China University of Mining and Technology, Xuzhou 221116, Jiangsu, China

[2] School of Chemical Engineering and Technology, China University of Mining and Technology, Xuzhou 221116, Jiangsu, China

[3] School of Chemical Engineering and Energy, Zhengzhou University, Zhengzhou 450066, Henan, China

behavior of different concentration polyethylene glycol (PEG) solutions (having almost the same surface tension but with different dynamic viscosities.) on Teflon plates with different roughness using the Wilhelmy plate method. They found that the advancing contact angle was weakly dependent of capillary number and contact line velocity; however, the receding contact angle significantly decreased with increasing capillary number, and the contact angle hysteresis increased with increasing capillary number. After exploring the influence of roughness on hydrophobicity, they suggested that surface roughness played an important role in dynamic contact angle. Based on the experimental results, they demonstrated that the variation of receding contact angle with time followed the molecular-kinetic theory model (MKT), and obtained a power law relation between the receding contact angle and the capillary number. In addition, numerous spreading scaling laws are proposed based on the time dependence of the spreading radius or dimensionless spreading factor using the droplet spreading method. For example, the well-known Tanner law [18], $R(t) = At^{\alpha}$, is suitable to describe the dynamic wetting behavior of the completely wetting system. For the partially wetting system, de Ruijter et al. [19] proposed a three-stage spreading process for the spreading of a spherical droplet on an ideal horizontal solid substrate—in the early-time spreading stage, $R(t) \approx R_0 + bt$, and in the intermediate-time spreading stage, $R(t) \sim t^{0.1}$, while in the long-time spreading stage until the equilibrium state is reached, $R(t) \approx R_{eq} - \exp(-t/T)$, where R_{eq} is the equilibrium spreading radius and T is a characteristic time constant. Wang et al. [20] proposed a reasonable exponential power law, $R(t) = R_{eq}[1 - \exp(-at^m/R_{eq})]$, to describe the case of partial wetting, where R_{eq} is the equilibrium spreading radius of drop and a is a coefficient. Typically, Lee et al. [21] experimentally explored the role of surface tension, viscosity, wettability, and surface roughness on the maximum spreading factor ($\beta_{max} = R_{max}/R_0$, where R_{max} is the maximum spreading radius, R_0 is the initial droplet radius). They found that the liquid properties (surface tension and viscosity) had a significant impact on the maximum spreading factor, while the dynamic wettability and the maximum spreading factor at low impact velocity was weakly dependent of surface roughness and type of surface (steel, aluminum, and parafilm). Based on these results mentioned above, an improved energy balance model for maximum spreading factor was proposed based on a correct analytical modeling of the time at maximum spreading. Up to now, wetting characteristics have been explored through different methods, but there are few literatures to study the same wetting system using different methods, which is very meaningful because different methods have different characteristics. To better understand the wetting mechanism, we studied the dynamic wetting behavior of deionized water and oleic acid on smooth Teflon surfaces using the Wilhelmy plate–dipping method and the droplet-spreading method, respectively.

Experimental section

Materials and cleaning procedure

Oleic acid (purity > 99%, AR) was purchased from Sinopharm Chemical Reagent Co., Ltd. (Shanghai, China). The physical parameters of oleic acid and deionized (DI) water are presented in Table 1. Teflon plates were purchased from http://www.tedpella.com which provided the microscopy products for science and industry. The morphology of Teflon was evaluated using an atom force microscope (AFM), as shown in Fig. 1. The consistency of Teflon was evaluated by measuring the equilibrium contact angle of DI water on different spots of randomly selected plates using DSA100 (KRÜSS, Germany) goniometer, and the average equilibrium contact angle was 115.5° ± 2°, which indicated that these plates were homogeneous for the study of wettability. In addition, the average equilibrium contact angle of oleic acid on Teflon was also determined at 57.5° ± 2°. All Teflon plates were carefully cleaned before the experiment, and the detailed information on the cleaning procedure could be found in the reference [22]. After cleaning, these plates were used to perform the forced spreading experiment and the spontaneous spreading experiment.

Forced spreading experiment apparatus

Forced spreading experiments were conducted using the Wilhelmy plate–dipping method with the MiniLab ILMS (GBX, France). ILMS mainly consists of a high-precision force sensor (used to determine the force exerted by liquids on the plate surface), a motorized microdisplacement platform (used to hold the liquid vessel and move it up and down at a specific speed), a video camera, a LED light source, and a data

Table 1 Physical parameters of oleic acid and deionized (DI) water used in this study

Reagents	Molecular weight (g/mol)	Density (kg/m^3)	Viscosity (mPa s)	Surface tension (mN/m)	Capillary length (mm)
Oleic acid	282.47	891	17.64	33.8	1.97
DI water	18.02	998	0.89	72.8	2.73

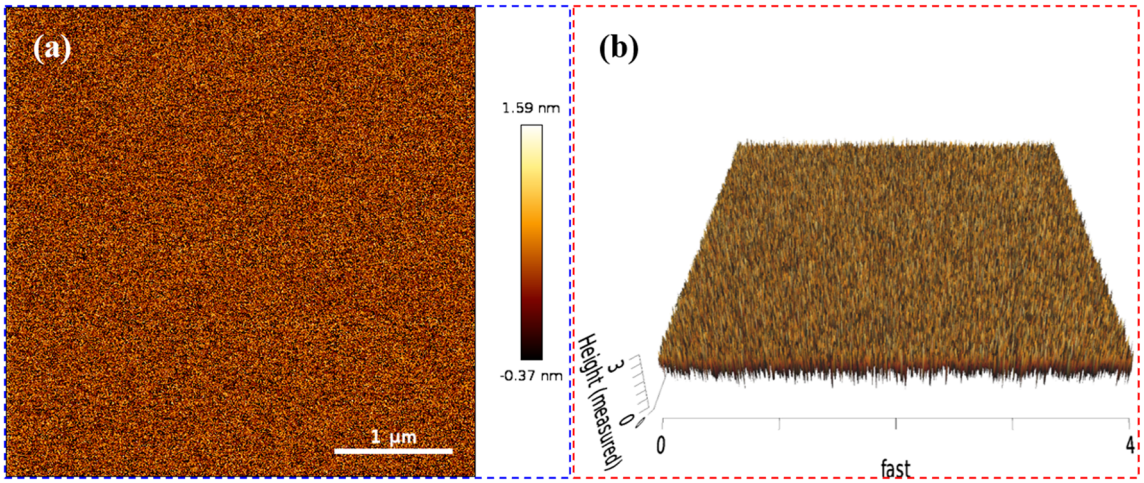

Fig. 1 **a** Two-dimensional and **b** three-dimensional morphology of Teflon

acquisition and processing system, its physical diagram and schematic diagram, and the force analysis of the plate during advancing/receding movement in a liquid pool are shown in Fig. 2. This apparatus uses the force balance method to measure dynamic contact angle at the three-phase contact line during the immersion/withdrawal of the plate in the pool of liquid. The forces applied on the plate during its motion include gravitational force (F_g), buoyancy force (F_B), capillary force (F_σ), and the mechanic force (F) from the plate holder on the plate being measured by the force sensor. Note that the gravitational force is calibrated at the onset of contact of the plate with the liquid. Therefore, the steady motion of the solid plate in the liquid pool is controlled by the abovementioned forces excluding the gravitational force, and finally, the dynamic contact angle is determined based on the principle of force balance. Readers interested in the force analysis of the plate in the liquid pool are recommended to refer to Karim et al. [17, 23]. Although one thinks that the tensiometric method is an indirect method of contact angle measurement, it is one of the most accurate methods for determining the small changes in contact angle [24]. It is noteworthy that the Wilhelmy plate method does not consider viscous force in the force balance equation to measure dynamic contact angle, which leads to significant errors in the measurement, especially for high-viscosity liquids and/or high contact line speeds [25, 26]. However, these errors can be neglected for the cases with low-viscosity liquids and low-speed of the contact line [25]. In this study, due to the low viscosity of the studied liquid and the low contact linear velocity, this apparatus can provide accurate dynamic contact angle measurement results.

The measurement procedure is as follows: first of all, the studied plate is fixed using a holder and suspended vertically on the honk of force sensor. Secondly, the desired volume of liquid is poured into the vessel and placed it on the microdisplacement platform; at this moment, the platform should be adjusted to the specified zero point. Then, with the help of the motor, the platform starts to move upward (advancing) until the liquid comes into direct contact with the plate. The liquid vessel then moves at a given speed until the plate reaches the immersion depth (10 mm in this study).

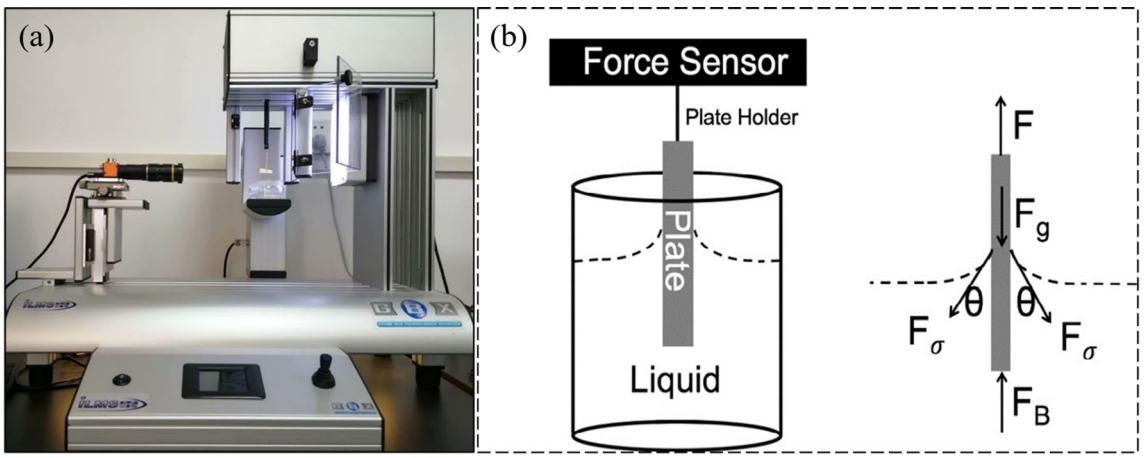

Fig. 2 **a** Physical diagram of MiniLab ILMS and **b** its schematic diagram and force analysis of the plate during advancing/receding movement in a liquid pool [17]

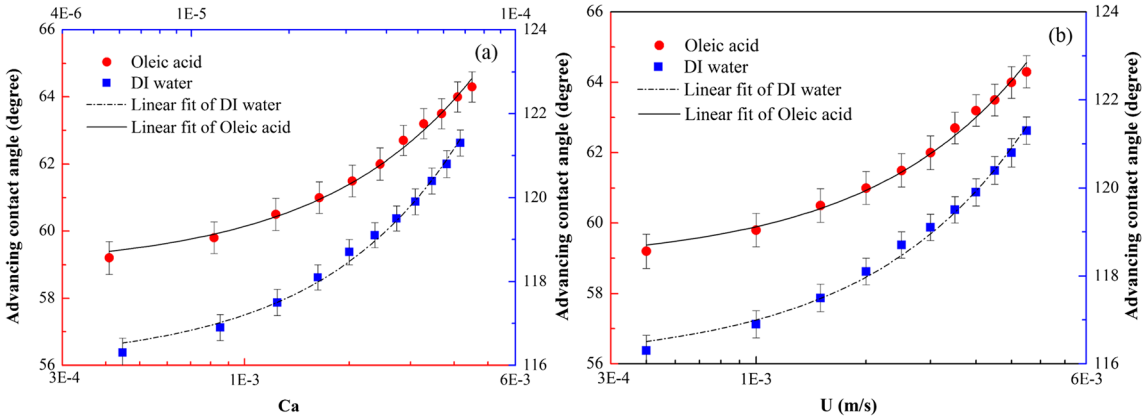

Fig. 3 Variation of advancing contact angle with capillary number (**a**) and contact line velocity (**b**) during the forced spreading of DI water and oleic acid on Teflon

After waiting for 1 s, the platform moves downward (receding) at the same speed. To ensure the accuracy of experimental results, each test was repeated at least three times, and new plates and fresh liquid were used to minimize potential contamination. All measurements were conducted at room temperature (around 25°), and relatively humidity RH = 40 ± 5%.

Spontaneous spreading experiment apparatus

Spontaneous spreading experiments were performed using the sessile drop method with the DSA100 (KRÜSS, Germany) goniometer. DSA100 allows us to observe and analyze the spreading behavior of liquid droplets over solid surfaces; its schematic diagram and the detailed operation procedure can be found in the reference [27]. Note that the liquid droplets could be considered as spheres before contact with the substrate because the size of the droplet was much smaller than the capillary length, so the gravity effect could be negligible compared with the effect of surface tension.

Results and discussion

Forced spreading experiments

In this section, we systematically investigated the forced spreading dynamics of DI water and oleic acid on smooth Teflon surfaces using the Wilhelmy plate–dipping method, and presented the variations of advancing contact angle, receding contact angle and contact angle hysteresis with capillary number ($Ca = \mu U/\gamma_{lv}$, where μ is the liquid viscosity, U is the contact line velocity, and γ_{lv} is the gas-liquid interfacial tension), and contact line velocity (U) for various wetting systems (i.e., DI water–Teflon system and oleic acid–Teflon system). Note that the data are presented in a log-log plot, and the error bar shown for the data represents the range of the data for the 3 runs conducted at each capillary number or contact line velocity. Figure 3 shows the advancing contact angle during the forced spreading of DI water and oleic acid on Teflon versus the contact line velocity ($5.0 \times 10^{-4} \le U \le 5.5 \times 10^{-3}$ m/s) and the capillary number ($6.0 \times 10^{-6} \le Ca \le 7.0 \times 10^{-5}$ for DI water and $4.0 \times 10^{-4} \le Ca \le 4.5 \times 10^{-3}$ for oleic

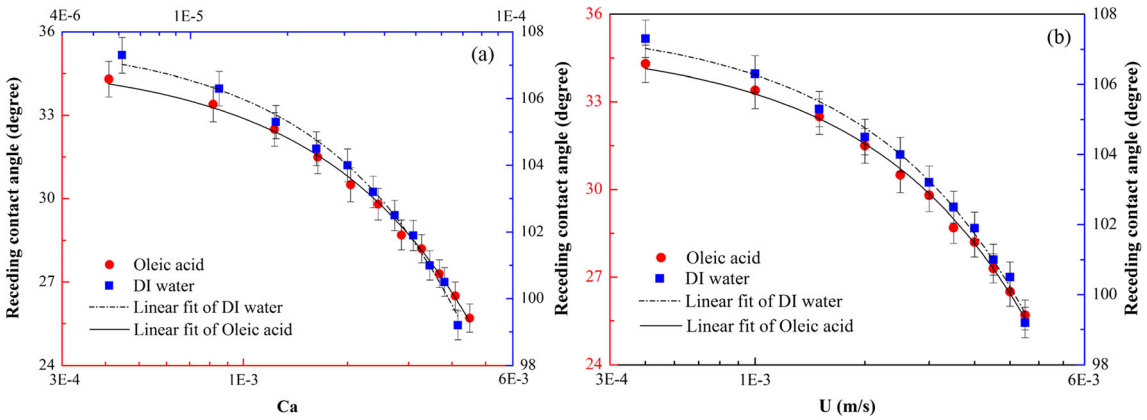

Fig. 4 Variation of receding contact angle with capillary number (**a**) and contact line velocity (**b**) during the forced spreading of DI water and oleic acid on Teflon

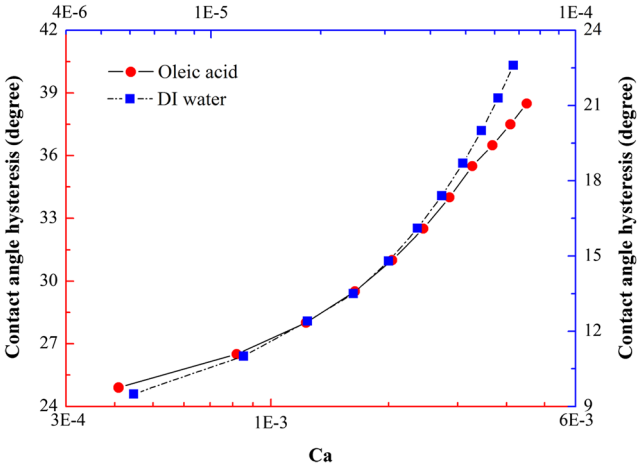

Fig. 5 Variation of contact angle hysteresis with capillary number during the forced spreading of DI water and oleic acid on Teflon

acid), respectively. The results showed a monotonic increase in the advancing contact angle with increasing *Ca* and *U* for all the wetting systems studied. Moreover, the advancing contact angle was found to be linearly dependent on the capillary number and the contact line velocity within the studied range of the capillary number and the contact line velocity, which is consistent with Karim et al. [17] and Kim et al. [28].

Figure 4 shows the receding contact angle during the forced spreading of DI water and oleic acid on Teflon versus the capillary number and the contact line velocity within the same studied range as the advancing contact angle, respectively. The results showed that the receding contact angles of all the studied liquids continued to decrease with the increase of capillary number and contact line velocity within the studied range, and the receding contact angle had a linear relationship with capillary number and three-phase contact linear velocity, which was in agreement with Karim et al. [17].

Contact angle hysteresis is defined as the difference between the advancing contact angle and the receding contact angle, and is plotted with capillary number, as shown in Fig. 5. As capillary number increased, the contact angle hysteresis increased for all the studied wetting systems. From the measurements in the literature, the contact angle hysteresis (20~60°) for the dynamic wetting system of water-smooth Teflon could be easily obtained at low capillary number region [28]. However, in this study, little contact angle hysteresis was achieved for the DI water–Teflon system, which could be attributed to the small capillary number due to the low viscosity and high surface tension of DI water and the limitation of the velocity of three-phase contact line. Interestingly, under the same experimental conditions, the hysteresis of contact angle of the oleic acid–Teflon system was much larger than that of the DI water–Teflon system. This could be considered as the result of two factors. First, compared with DI water–Teflon system, the oleic acid–Teflon system has larger capillary number due to higher viscosity and lower surface tension of oleic acid. Because the larger the capillary number, the more significant the contact angle hysteresis phenomenon. Second, the surface of Teflon exhibits hydrophobicity properties, and the oleic acid molecules easily adsorb on the surface of Teflon resulting in the formation of an oil film on the surface during the receding of contact line. As a result, the receding contact angle of oleic acid on Teflon reduced; therefore, the contact angle hysteresis increased.

To investigate the scaling behaviors of advancing contact angles, the difference between the cube of dynamic advancing contact angles (θ_A) and static equilibrium contact angles (θ_e) was calculated and plotted against capillary number in Fig. 6.

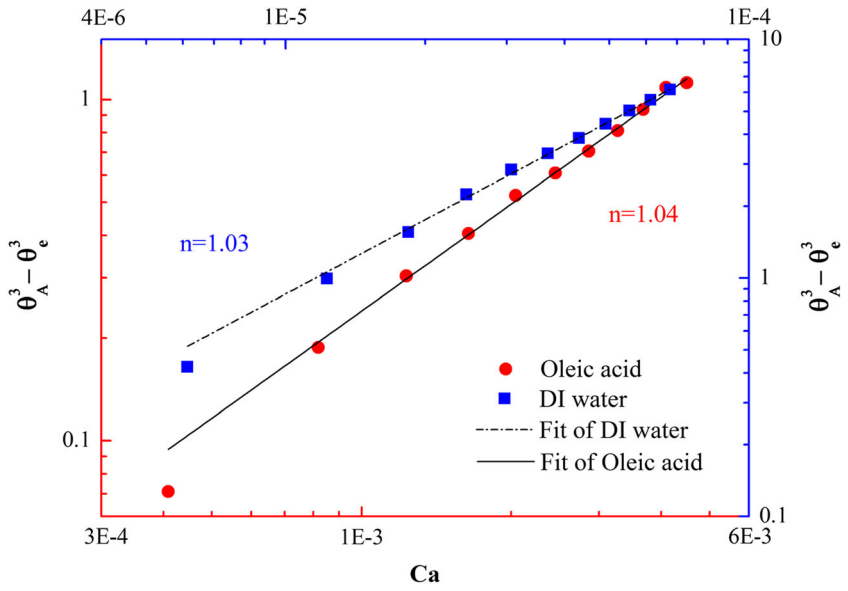

Fig. 6 Relationship between $(\theta_A^3-\theta_e^3)$ and capillary number during the forced spreading of DI water and oleic acid on Teflon

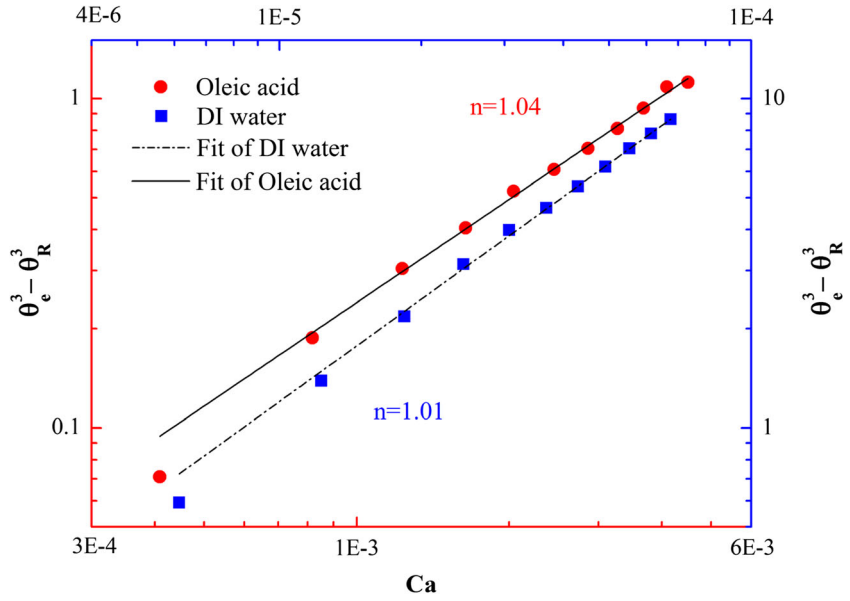

Fig. 7 Relationship between $(\theta_e^3-\theta_R^3)$ and capillary number during the forced spreading of DI water and oleic acid on Teflon

Results showed that the relationship between $\theta_A^3-\theta_e^3$ and Ca was found to follow the power law: $(\theta_A^3-\theta_e^3)\sim Ca^n$, which was similar to Karim et al. [17], where n is the slope of line in the log-log plot shown in Fig. 6. It is obvious that n is almost 1 for all the wetting systems studied, which is reasonable because when $Ca < 0.001$, $n = 1$ [17]. Since $n = 1$, we could conclude that the variation of $\theta_A^3-\theta_e^3$ with Ca followed the Cox-Voinov-Tanner's scaling law, $\theta_A^3-\theta_e^3 \propto Ca$, which is consistent with Kim et al. [29]. In addition, we also studied the scaling behaviors of receding contact angles, as shown in Fig. 7. It is clear that $\theta_e^3-\theta_R^3$ increased linearly with the rise of Ca, and the relationship between them also followed the Cox-Voinov-Tanner's scaling law.

Spontaneous spreading experiments

This section studied the spontaneous spreading dynamics of DI water and oleic acid on smooth Teflon surfaces through the change of dynamic contact angle and spreading radius using the droplet spreading method. Note that the data are presented in a log-log plot, and the error bar shown for the data represents the range of the data for the 3 runs. The variations of dynamic contact angle (a) and spreading radius (b) with time during the spontaneous spreading of DI water and oleic acid on Teflon are presented in Fig. 8. Results showed that for all the wetting systems studied the dynamic contact angle continued to decrease with time until the equilibrium value was reached, while the spreading radius showed an opposite trend. To better describe the spontaneous spreading dynamics, we have carried out empirical fitting on the experimental data, and found that the variation of dynamic contact angle with time for all the wetting systems studied could be well described by the expression, $\theta(t) = \theta_{eq} + a * \exp(-t/m)(a > 0)$. And the nonlinear fitting generated R^2 values of 0.998 and 0.992 for the oleic acid–Teflon system and the DI water–Teflon system, respectively. In a similar way, we found that the dependence of the spreading radius on time could be well described by the expression, $R(t) = R_{eq} + a * \exp(-t/m)(a < 0)$, and generated R^2 values of 0.998 and 0.997 for the oleic acid–

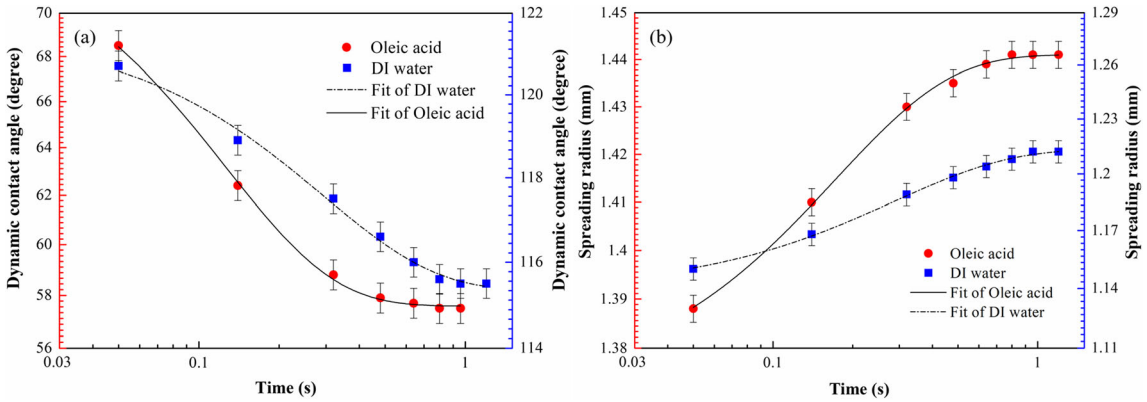

Fig. 8 Variation of dynamic contact angle (**a**) and spreading radius (**b**) with time during the spontaneous spreading of DI water and oleic acid on Teflon

Teflon system and the DI water–Teflon system, respectively. According to de Ruijter et al. [19], the whole spreading process of a spherical droplet on an ideal horizontal solid surface for the partial wetting system could be separated into three stages: the early-time spreading stage described by $R(t) \approx R_0 + bt$, the intermediate-time spreading stage expressed by $R(t) \approx t^{0.1}$, and the long-time spreading stage (including the equilibrium state) described by $R(t) \approx R_{eq} - \exp(-t/T)$, where R_{eq} is the equilibrium spreading radius and T is a characteristic time constant. Obviously, de Ruijter's model could describe the whole spreading process in detail, but only the similar law of the long-time spreading stage could perfectly fit our experimental data. This was mainly attributed to the limitations of camera, which made us only study the time scale from hundreds of milliseconds to dozens of seconds. The current results mean that we must use high-speed photography technology to deeply study the spontaneous spreading phenomenon, because the spreading of liquid droplets on a solid surface usually happens in the time range from milliseconds to seconds [30], especially the duration of the early spreading stage is very short, about a few milliseconds.

Conclusion

The dynamic wetting behavior of DI water and oleic acid on smooth Teflon surfaces was studied using the Wilhelmy plate–dipping method and the droplet-spreading method, respectively. The Wilhelmy plate–dipping method was based on the principle of force balance to measure dynamic contact angle at the three-phase contact line during the immersion (advancing) and emersion (receding) of the plate in the pool of liquid. Our work suggested that the advancing contact angle increased monotonically with the rise of capillary number and contact line velocity within the studied range, while the receding contact angle exhibited an opposite trend; therefore, the contact angle hysteresis defined as the difference between the advancing contact angle and the receding contact angle was dependent of capillary number. Besides, the scaling behaviors of advancing contact angle and receding contact angle were found to follow Cox–Voinov–Tanner's scaling law. The droplet spreading method allowed us to observe and analyze the spreading behavior of liquid droplets over solid surfaces; however, due to the limitations of camera, we only investigated the spontaneous spreading dynamics of the long-time spreading stage, and found that the variations of dynamic contact angle and spreading radius with time could be well described by the expressions, $\theta(t) = \theta_{eq} + a * \exp(-t/m)\ (a > 0)$ and $R(t) = R_{eq} + a * \exp(-t/m)(a < 0)$, respectively.

Author contributions The manuscript was written through contributions of all authors. All authors have given approval to the final version of the manuscript.

Funding information This work was supported by the National Nature Science Foundation of China (U1704252; 51904299) and the Fundamental Research Funds for the Central Universities (2019XKQYMS62) for which the authors express their appreciation.

Compliance with ethical standards

Conflict of interest The authors declare that they have no competing interests.

References

1. Watson GS, Gellender M, Watson JA (2014) Self-propulsion of dew drops on lotus leaves: a potential mechanism for self-cleaning. Biofouling 30:427–434
2. Zheng Y, Gao X, Jiang L (2007) Directional adhesion of superhydrophobic butterfly wings: a superhydrophobic state with high adhesive force. Soft Matter 3:178–182
3. Zheng Y, Bai H, Huang Z, Tian X, Nie F, Zhao Y, Zhai J, Jiang L (2010) Directional water collection on wetted spider silk. Nature 463:640–643
4. Sherbrooke WC, Scardino AJ, Nys RD, Schwarzkopf L (2007) Functional morphology of scale hinges used to transport water: convergent drinking adaptations in desert lizards (moloch horridusandphrynosoma cornutum). Zoomorphology 126:89–102
5. Si Y, Yu C, Dong Z, Jiang L (2018) Wetting and spreading: fundamental theories to cutting-edge applications. Curr Opin Colloid Interface Sci 36:10–19
6. Shen Y, Tao J, Tao HJ, Chen S, Pan L, Wang T (2015) Relationship between wetting hysteresis and contact time of a bouncing droplet on hydrophobic surfaces. ACS Appl Mater Interfaces 7:20972–20978
7. Sarkar A, Kietzig AM (2013) General equation of wettability: a tool to calculate the contact angle for a rough surface. Chem Phys Lett 574:106–111
8. Koishi T, Yasuoka K, Fujikawa S, Zeng XC (2011) Measurement of contact-angle hysteresis for droplets on nanopillared surface and in the cassie and wenzel states: a molecular dynamics simulation study. ACS Nano 5:6834–6842
9. Ranabothu SR, Karnezis C, Dai LL (2005) Dynamic wetting: hydrodynamic or molecular-kinetic? J Colloid Interface Sci 288:213–221
10. Arjmandi-Tash O, Kovalchuk NM, Trybala A, Kuchin IV, Starov V (2017) Kinetics of wetting and spreading of droplets over various substrates. Langmuir 33:4367–4385
11. Semenov S, Trybala A, Rubio RG, Kovalchuk N, Starov V, Velarde MG (2014) Simultaneous spreading and evaporation: recent developments. Adv Colloid Interf Sci 206:382–398
12. Minaki H, Li S (2014) Multiscale modeling and simulation of dynamic wetting. Comput Methods Appl M Eng 273:273–302
13. Cox RG (1986) The dynamics of the spreading of liquids on a solid surface. Part 1. Viscous flow. J Fluid Mech 168:195–220
14. Voinov OV (1976) Hydrodynamics of wetting. Fluid Dynam 11:714–721
15. Blake TD, Haynes JM (1969) Kinetics of liquid/liquid displacement. J Colloid Interface Sci 30:421–423
16. Petrov P, Petrov I (1992) A combined molecular-hydrodynamic approach to wetting kinetics. Langmuir 8:1762–1767
17. Karim AM, Rothstein JP, Kavehpour HP (2018) Experimental study of dynamic contact angles on rough hydrophobic surfaces. J Colloid Interface Sci 513:658–665

18. Kovalchuk NM, Barton A, Trybala A, Starov V (2015) Mixtures of catanionic surfactants can be superspreaders: comparison with trisiloxane superspreader. J Colloid Interface Sci 459:250–256
19. De Ruijter MJ, De Coninck J, Oshanin G (1999) Droplet spreading: partial wetting regime revisited. Langmuir 15:2209–2216
20. Wang XD, Zhang Y, Lee DJ, Peng XF (2007) Spreading of completely wetting or partially wetting power-law fluid on solid surface. Langmuir 23:9258–9262
21. Lee JB, Derome D, Guyer R, Carmeliet J (2016) Modeling the maximum spreading of liquid droplets impacting wetting and nonwetting surfaces. Langmuir 32:1299
22. Wang J, Cao Y, Xing Y, Li G, Liao Y, Li S, An M (2019) Spreading behavior of oil droplets over polytetrafluoroethylene plates in deionized water. J Disper Sci Technol. https://doi.org/10.1080/01932691.2019.1645025
23. Karim AM, Davis SH, Kavehpour HP (2016) Forced versus spontaneous spreading of liquid. Langmuir 32:10153–10158
24. Alghunaim A, Kirdponpattara S, Newby BMZ (2016) Techniques for determining contact angle and wettability of powders. Powder Technol 287:201–215
25. Karim AM, Kavehpour HP (2018) Effect of viscous force on dynamic contact angle measurement using Wilhelmy plate method. Colloids Surf A Physicochem Eng Asp 548:54–60
26. Zhang P, Mohseni K (2019) Viscous drag force model for dynamic Wilhelmy plate experiments. Phys Rev Fluids 4:084004
27. Wang J, Cao Y, Li G, Zou Y, Hao X (2019) Spreading kinetics of oil droplets over three different substrates. Energy Source Part A. https://doi.org/10.1080/15567036.2019.1643951
28. Kim JH, Kavehpour HP (2015) Dynamic contact angle measurements on superhydrophobic surfaces. Phys Fluids 27:032107
29. Kim JH, Rothstein JP (2015) Dynamic contact angle measurements of viscoelastic fluids. J Non-Newton Fluid Mech 225:54–61
30. Shi L, Liu Y, Lu H, Meng Y, Hu G, Tian Y (2017) Viscous force retards initial droplet spreading. J Phys Chem C 121:22054–22059